

Control the GNN: Utilizing Neural Controller with Lyapunov Stability for Test-Time Feature Reconstruction

Jielong Yang, Rui Ding, Feng Ji, Hongbin Wang, Linbo Xie

Abstract

The performance of graph neural networks (GNNs) is susceptible to discrepancies between training and testing sample distributions. Prior studies have attempted to enhance GNN performance by reconstructing node features during the testing phase without modifying the model parameters. However, these approaches lack theoretical analysis of the proximity between predictions and ground truth at test time. In this paper, we propose a novel node feature reconstruction method grounded in Lyapunov stability theory. Specifically, we model the GNN as a control system during the testing phase, considering node features as control variables. A neural controller that adheres to the Lyapunov stability criterion is then employed to reconstruct these node features, ensuring that the predictions progressively approach the ground truth at test time. We validate the effectiveness of our approach through extensive experiments across multiple datasets, demonstrating significant performance improvements.

Introduction

Graph neural networks (GNNs) have gained significant attention in recent years due to their strong representational capabilities (Wu et al. 2020; Yuan et al. 2022). As the applications and data scales of GNNs continue to grow, their performance becomes sensitive to discrepancies between training and testing sample distributions (Qin et al. 2022; Li et al. 2022). To address performance degradation caused by distribution shift, some approaches enhance the model's generalization during the training phase using techniques such as data augmentation (Sui et al. 2024; Ding et al. 2022), causal inference (Fan et al. 2023), and regularization (Buffelli, Liò, and Vandin 2022). However, these techniques require modifications to the model structure or parameters, limiting their applicability when the model architecture is fixed or when retraining is prohibitively expensive.

To improve the practicality of graph neural networks, some approaches focus on reconstructing node features during the testing phase to enhance model performance without altering parameters. Well-designed perturbations to GNN input data (Jin et al. 2023) is introduced to reduce the effects of distribution shift, guided by a surrogate loss. However, this method results in node features with low feasibility. To address this, FRGNN (Ding et al. 2024) employs an MLP

to learn the mapping between GNN outputs and inputs, generating class representative embeddings for each node class during the testing phase. Then FRGNN replaces the features of known label nodes with these class representative embeddings to enhance model robustness against distribution shift. Despite their effectiveness, this method relies on manually designed rules or mechanisms for node feature reconstruction and lacks theoretical analysis of the proximity between predictions and ground truth at test time.

To improve the feasibility of feature reconstruction methods during the testing phase, we formalize GNNs as control systems, treating node features as controlled variables and the predictions as state. The aforementioned methods can be viewed as solving an optimization problem, specifically finding a node feature that minimizes the discrepancy between the GNN's prediction and the ground truth. Transforming this problem into a control problem offers the following advantages:

- Compared to the approaches of optimizing a single loss function, this method offers more precise control over each individual state.
- Introducing a control system allows the use of stability criteria from control theory to analyze the stability of the system, determining whether the system output remains stable near the equilibrium point.

Our goal is to find a controller to ensure the predictions get close to the ground truth gradually. However, due to the complex nonlinearity of GNNs, traditional controllers face significant challenges in meeting the control requirements. Methods like the proportional–integral–derivative controller (PID) (Ang, Chong, and Li 2005) and the linear quadratic regulator (LQR) (Kwakernaak and Sivan 1972) are widely used in various fields. However, the control effectiveness of these methods for nonlinear systems is relatively poor. In contrast, model-free adaptive control (MFAC) (Hou and Xiong 2019) has superior capability in handling nonlinear dynamics. But unlike ordinary neural networks like MLPs, GNNs include a message-passing layer. Adjusting the features of specific nodes affects not only the output of those nodes but also influences the prediction outputs of other nodes through the graph structure. This interdependence makes the control problem more complex and challenging for such controllers. To tackle this issue, we introduce a neu-

ral controller. Neural controllers have been successfully used in various tasks, including inverted pendulum and drone control (Jiang, Pourpanah, and Hao 2020; Kim and Calise 1994; Gu et al. 2020). To ensure stability, some studies have proposed neural Lyapunov functions for neural controllers (Chang, Roohi, and Gao 2020; Zhou et al. 2022; Dai et al. 2021). However, these approaches are focused on traditional control problems and have not been applied to the node feature reconstruction problem in GNNs.

To broaden the application scope of neural controllers, we apply them to the node feature reconstruction in graph neural networks. We utilize neural controllers to adjust node features and learn controller parameters in a data-driven manner. This method aims to control the node’s predicted output to the ground truth gradually. To ensure that the node prediction output remains stable near the ground truth, we require the learned neural controller to satisfy the Lyapunov stability criterion. Since it is challenging to design Lyapunov functions for complex controllers manually, we introduce a neural Lyapunov function to approximate the Lyapunov function through a neural network. We simultaneously learn the parameters of the neural controller and the neural Lyapunov function to ensure that the controller satisfies the Lyapunov criterion under this Lyapunov candidate, thereby ensuring the stability of the control system. Our contributions are summarized as follows:

- We propose a new paradigm for applying control theory to enhance the performance of graph neural networks. We formalize the GNN as a control system, considering node features as controlled variables and the predictions as state. We design controllers to optimize these variables to improve model prediction results.
- We design a neural controller suitable for the performance enhancement tasks of graph neural networks. To ensure that the controller can effectively adjust node features, we introduce a neural Lyapunov function. By ensuring the validity of this Lyapunov function, we guarantee the stability of the controller.
- We validate the effectiveness of our method on multiple datasets. Experimental results demonstrate that our approach significantly enhances the performance of graph neural networks by mitigating the impact of distribution shift, all without altering the model parameters.

Related Work

Test-Time Feature Reconstruction For GNNs

In the task of semi-supervised node classification, GNNs often suffer from a distribution shift between the training set and testing set due to the inappropriate selection of training samples or limited training data. To tackle this issue without altering the model structure and parameters, reconstructing node features during the testing phase is effective. GTrans (Jin et al. 2023) employs surrogate loss to guide the update of perturbations during the testing phase to reconstruct node features. FRGNN (Ding et al. 2024) proves that replacing the node features of labeled nodes with class representative embeddings during the testing phase enhances

the model’s robustness to distribution shift. Identifying appropriate class representative embeddings is crucial for this method. FRGNN maps the relationship between GNN outputs and inputs using an MLP. Then, it uses the one-hot embedding of the class as input to the MLP to obtain the class representative embeddings. However, the class representative embeddings obtained in this way do not guarantee that the new output of GNN will be close to the one-hot embedding of the corresponding class, which fails to meet the requirements of class representative embeddings. To address this issue, we design a neural controller to find appropriate class representative embeddings by ensuring that the new prediction of GNN gets close enough to the ground truth.

Neural Controller and Neural Lyapunov Function

Lyapunov stability is commonly used in control theory to ensure system stability. However, designing Lyapunov functions of neural controllers is challenging. To address this issue, (Chang, Roohi, and Gao 2020) presents a learning framework to learn control policies and their corresponding Lyapunov functions. This framework guides model training by continuously searching for counterexamples that do not satisfy the Lyapunov condition until all states in the domain satisfy the Lyapunov condition. However, this method requires the Lyapunov function to be differentiable for counterexample search with the SMT solvers. To meet this requirement, all activation functions in (Chang, Roohi, and Gao 2020) are Tanh. To relax the restriction that the activation function must be continuous, (Dai et al. 2021) proposes using Mix Integer Programs (MIP) to find counterexamples. This method allows the widely used ReLU activation function to be used. The authors rigorously prove the validity of the Lyapunov function. (Zhou et al. 2022) learns the unknown nonlinear system through a neural network without the need for precise system modeling. Then, the system is controlled using the framework proposed in (Chang, Roohi, and Gao 2020). The authors theoretically guarantee the validity of the Lyapunov function under the unknown system. Although these methods simplify the design of Lyapunov functions, they solve traditional control problems rather than enhancing the neural networks’ performance with Lyapunov functions. Our work is inspired by these studies. We design a neural controller to reconstruct node features to improve model prediction.

Methodology

In this section, we introduce the method of reconstructing node features using a neural controller. The overall process of this method is shown in Figure 1. Initially, we use a well-trained GNN to obtain the node predictions. This output is then fed back into the neural controller to reconstruct the node features, ensuring the new predictions remain close to the ground truth. To ensure that the new predictions derived from the reconstructed node features remain stable near the ground truth, we introduce a neural Lyapunov function to aid in controller training. This section is organized as follows. We first explain the theoretical foundation of this method. Then, we detail the design of the neural controller and the

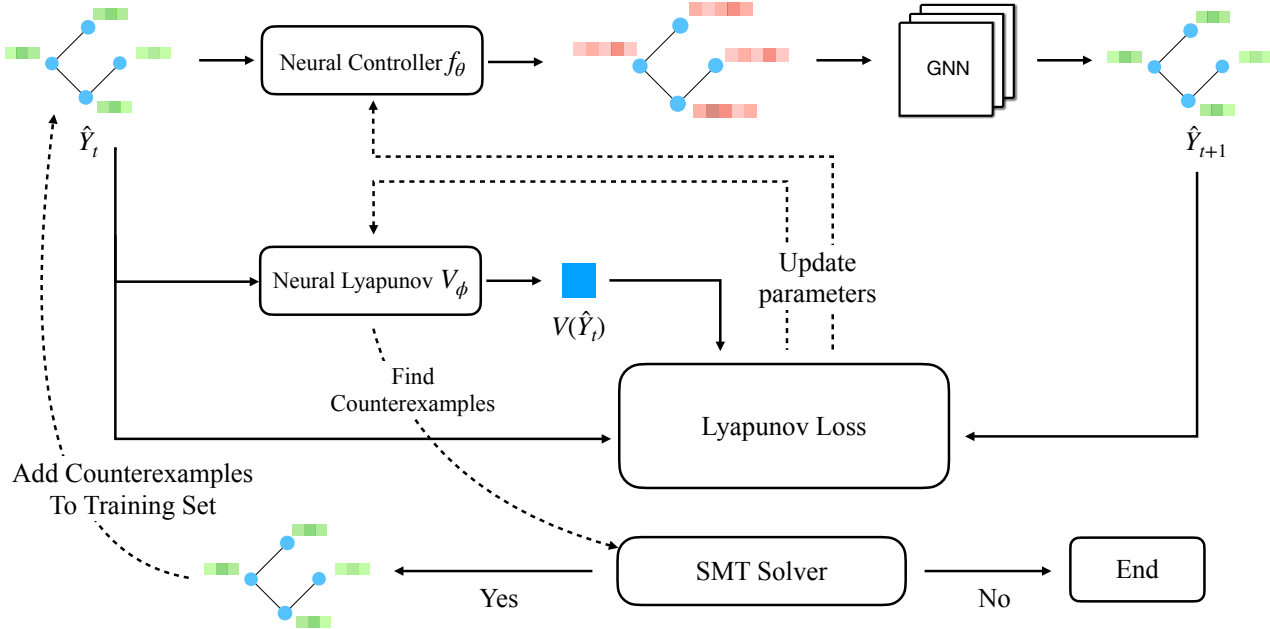


Figure 1: The overall process of our method.

neural Lyapunov function. Finally, we outline the training approach for this neural controller and the neural Lyapunov function.

Problem Formulation

In FRGNN (Ding et al. 2024), the authors demonstrate that replacing the features of labeled nodes with class representative embeddings during the test phase can improve the model's robustness to distribution shift. This paper provides the definition of class representative embeddings, as shown in Definition 1.

Definition 1 *Class Representative Embedding $h_{c_i}^*$:* Suppose the embedding $h_{c_i}^*$ of node i with label c_i satisfies the following conditions:

$$\|C(h_{c_i}^*) - c_i\|_2 \leq \epsilon, \quad (1)$$

where C represents the trainable classifier in GNNs and ϵ denotes a small positive number. Then $h_{c_i}^*$ is defined as the class representative embedding of class c_i .

We draw inspiration from the definition in FRGNN, aiming to identify class representative embeddings with theoretical guarantees. The inference process of the graph neural network is as follows:

$$\hat{Y} = \text{GNN}(X, A) = C(g(X, A)), \quad (2)$$

where \hat{Y} represents the node predictions, X denotes the node features, A is the adjacency matrix of the graph, GNN represents a well-trained graph neural network, g denotes any aggregation function, and C represents the trainable classifier, such as MLP. Our goal is to reconstruct the node features X based on the existing predictions \hat{Y} to ensure

that the new predictions get close to the ground truth. This reconstruction process is denoted as f . Formally, this can be written as the following optimization problem:

$$\min_f \|C(f(g(X, A), \hat{Y})) - Y\|_2, \quad (3)$$

where f represents a function. Our goal is to identify a function f to minimize the objective function in Equation (3). However, solving this optimization problem is challenging due to the complex nonlinearity of GNNs. We reanalyze the problem. Considering the advantages of converting the optimization problem into a control problem mentioned in our introduction, we transform the optimization challenge into a control problem. We can formalize the graph neural network as a control system, treating node features as controlled variables and the predictions as states. By designing a controller to adjust these controlled variables, we aim to ensure that the node predictions get close to the ground truth, thereby enhancing the model's performance. The form of this control system is as follows:

$$\hat{Y}_{t+1} = C(f(g(X, A), \hat{Y}_t)), \quad (4)$$

where \hat{Y}_t represents the predictions at time t , and \hat{Y}_{t+1} represents the predictions at time $t + 1$. This control system feeds back the predictions at time t to the controller f . Then the controller f adjusts the node features to ensure that the subsequent predictions at time $t + 1$ get close to the equilibrium point, which is the ground truth. Since GNN is fixed and thus $g(X, A)$ is constant, Equation (4) can be viewed as a function of the variable \hat{Y}_t , as shown below:

$$\hat{Y}_{t+1} = C(f(\hat{Y}_t)). \quad (5)$$

We have now transformed the optimization problem in Equation (3) into designing a controller f . We aim to ensure that the controller f satisfies the Lyapunov stability criterion, ensuring that the system output remains stable near the equilibrium point (i.e., ground truth).

Theoretical Foundation

In the previous chapter, we transform the GNNs optimization problem into a control problem. Now, the main challenge is designing a controller f to adjust the node features so that the new predictions derived from these reconstructed features get close to the ground truth. Traditional controllers, such as PID, LQR, and AC, are not well-suited for this system due to the complex nonlinearity of graph neural networks. Moreover, unlike ordinary neural networks like MLPs, GNNs include message-passing layers, meaning that modifying a specific node feature not only affects the prediction of that node but also influences the predictions of other nodes through the graph structure. This coupling makes the control problem particularly challenging for traditional controllers. Therefore, we choose a neural controller, leveraging the powerful representation capabilities of neural networks to learn an effective controller suitable for this system. We denote the neural controller as f_θ , where θ represents the trainable parameters. Thus, Equation (5) can be rewritten in closed-loop form as follows:

$$\hat{Y}_{t+1} = C(f_\theta(\hat{Y}_t)) \triangleq C_{f_\theta}(\hat{Y}_t). \quad (6)$$

To ensure the stability of this controller, we employ the Lyapunov stability theory. For a nonlinear closed-loop system, we can use Lyapunov stability criteria to determine system stability. This criterion leverages a scalar function $V(x)$ to assess system stability, known as the Lyapunov function. To apply the Lyapunov stability criterion to the closed-loop system in Equation (6), we introduce the following theorem.

Theorem 1 Consider a close-loop system $\hat{Y}_{t+1} = C_{f_\theta}(\hat{Y}_t)$ with an equilibrium point at the Y , i.e. $C_{f_\theta}(Y) = Y$, where C_{f_θ} is a MLP with ReLU activation function. Suppose there exists a continuously differentiable function $V : \mathbb{R}^n \rightarrow \mathbb{R}$ that satisfies the following conditions:

$$V(Y) = 0, \text{ and, } \forall \hat{Y} \in \mathcal{D} \setminus \{Y\}, V(\hat{Y}) > 0 \text{ and } \Delta V \leq 0. \quad (7)$$

where \mathcal{D} is the domain of the control system and ΔV is defined as:

$$\Delta V = V(C_{f_\theta}(\hat{Y}_t)) - V(\hat{Y}_t). \quad (8)$$

Then, the system is asymptotically stable at Y .

Proof 1 Please refer to the Appendix A.

Definition 2 Lyapunov Function: Any continuously differentiable function V maps the state space to a scalar value. **Lyapunov Stability Criterion:** For a close-loop system $\hat{Y}_{t+1} = C_{f_\theta}(\hat{Y}_t)$ with an equilibrium point at the Y , the system is asymptotically stable at the Y if there exists a Lyapunov function V that satisfies the conditions in Equation (7).

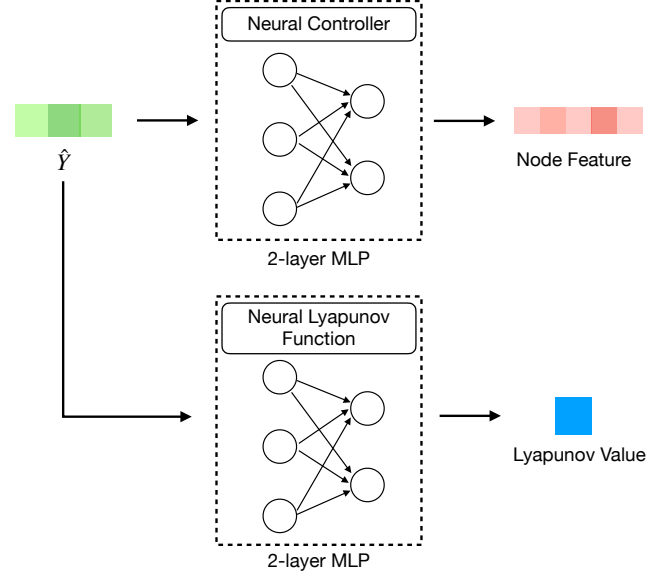


Figure 2: The architecture of the neural controller and the neural Lyapunov function.

Theorem 1 guarantees the stability of the system if the Lyapunov function V satisfies the conditions in Equation (7). Our objective is to identify a Lyapunov function V that satisfies Equation (7). However, designing a Lyapunov function for nonlinear systems is challenging. To address this issue, we introduce a neural Lyapunov function, which approximates the Lyapunov function through a neural network to derive a candidate Lyapunov function. We denote this learnable candidate neural Lyapunov function as V_ϕ , where ϕ represents the trainable parameters. The architecture of the neural network is illustrated in Figure 2. The neural Lyapunov function V_ϕ takes the predictions \hat{Y}_t at time t as input and outputs two components. The first component is the Lyapunov function $V_\phi(\hat{Y}_t)$, which is used to assess system stability. The second component is the output of the neural controller $f_\theta(\hat{Y}_t)$, which is used to adjust the node features.

Training Methodology

To obtain the candidate Lyapunov function V_ϕ for the neural controller f_θ , we need to train two neural networks simultaneously, one for the neural controller f_θ and the other for the neural Lyapunov function V_ϕ . Our objective is to find an f_θ that allows the system output to asymptotically stabilize at the equilibrium point (ground truth). The training goal is to ensure that all states \hat{Y} within the domain satisfy the Lyapunov stability criterion. To this end, we design the following Lyapunov loss function:

$$\mathcal{L}_{\phi, \theta} = \frac{1}{N} \sum_{i=1}^N (\sigma(-V_\phi(\hat{Y}_t^i)) + \sigma(\Delta V_\phi(\hat{Y}_t^i))) + V_\phi^2(Y), \quad (9)$$

where N represents the number of training samples, σ denotes the ReLU activation function, $\sigma(-V_\phi(\hat{Y}_t^i))$ ensures

that the neural Lyapunov function maps all states except the equilibrium point to positive values, satisfying the Lyapunov stability criterion $\forall x \in \mathcal{D} \setminus \{x_0\}, V(x) > 0$. $\sigma(\Delta V_\phi(\hat{Y}_i))$ ensures that the neural Lyapunov function has smaller values closer to the equilibrium point, satisfying the Lyapunov stability criterion $\Delta V \leq 0$. $V_\phi^2(Y)$ ensures that the Lyapunov function approaches zero at the equilibrium point, satisfying the Lyapunov stability criterion $V(x_0) = 0$.

The above process defines the training loss function, while we also need to design a method for obtaining training samples. Since the domain of the Lyapunov function is the entire state space, exploring every possible state is infeasible. Therefore, we use an analytical approach to identify counterexamples that violate the Lyapunov criteria within this domain, generating our training samples. Equation (7) defines the constraints that the Lyapunov function should satisfy. We take the negation of this equation to obtain states that violate the Lyapunov criterion. We define these states as follows:

$$\mathcal{C} = \{\hat{Y} | (V_\phi(\hat{Y}) \leq 0 \cup \Delta V_\phi(\hat{Y}) \geq 0) \cap \|\hat{Y}_i - Y_i\|_2 \geq \epsilon\}, \quad (10)$$

where Y is the equilibrium point and ϵ is a small positive number. The condition $V_\phi(\hat{Y}) \leq 0 \cup \Delta V_\phi(\hat{Y}) \geq 0$ restricts the found state \hat{y} from satisfying the conditions in Equation (7). The constraint $\|\hat{Y}_i - Y_i\|_2 \geq \epsilon$ ensures numerical stability. When the state is close to the equilibrium point, numerical calculations may become unstable, especially when using solvers to analyze system dynamics. By introducing this term, we ensure that the numerical solution does not produce large relative errors or numerical overflow when the state is close to zero. We utilize the satisfiability modulo theories (SMT) solver to solve this equation, obtaining states that violate the Lyapunov criterion. When the solver finds states that violate the Lyapunov criterion within the domain, we add these states as counterexamples to the training set for training the neural controller f_θ and the neural Lyapunov function V_ϕ . Our training process is detailed in Algorithm 1.

Test-Time Feature Reconstruction

After training the neural controller f_θ and the neural Lyapunov function V_ϕ , we can use the neural controller to adjust the node features during the testing phase. The inference formula is as follows:

$$\begin{aligned} h_{c_i}^* &= f_\theta(Y), \\ \hat{Y} &= \text{GNN}(r(h_{c_i}^*, X), A), \end{aligned} \quad (11)$$

where $h_{c_i}^*$ represents the class representative embedding of class c_i and r denotes the replacement function. The neural controller f_θ adjusts the node features to obtain the class representative embeddings $h_{c_i}^*$ and then we replace the features of labeled nodes with $h_{c_i}^*$. This process enhances the model's robustness to distribution shift.

Experiments

In this section, we evaluate our method across multiple datasets to demonstrate its effectiveness in reconstructing

Algorithm 1: Counterexample-Guided Neural Lyapunov Function Training

```

1: function TRAINING( $\hat{Y}, Y_i$ )
2:    $\Delta V_\phi = V_\phi(C(f_\theta(\hat{Y}))) - V_\phi(\hat{Y})$ 
3:    $\mathcal{L}_{\phi, \theta} = \frac{1}{N} \sum_{i=1}^N (\sigma(-V_\phi(\hat{Y}_i)) + \sigma(\Delta V_\phi(\hat{Y}_i))) + V_\phi^2(Y_i)$ 
4:    $\theta \leftarrow \theta - \alpha \nabla_\theta \mathcal{L}$ 
5:    $\phi \leftarrow \phi - \alpha \nabla_\phi \mathcal{L}$ 
6: return  $V_\phi, f_\theta$ 
7: end function
8:
9: function COUNTER GENERATION( $V_\phi, f_\theta$ )
10:   $\mathcal{C} = \{y | (V_\phi(y) \leq 0 \cup \Delta V_\phi(y) \geq 0) \cap \|y - Y_i\|_2 \geq \epsilon\}$ 
11:  Use SMT solver to find  $y$  that do not satisfy  $\mathcal{C}$ 
12: return Counterexamples  $y$ 
13: end function
14:
15: function MAIN
16:   Prepare close-loop system  $C$  and  $\hat{Y}$  derived from
      well-trained GNN
17:   Initialize  $V_\theta$  and initialize  $f_\theta$  randomly
18:   while True do
19:      $V_\phi, f_\theta \leftarrow \text{TRAINING}(\hat{Y}, Y_i)$ 
20:      $y \leftarrow \text{COUNTER GENERATION}(V_\phi, f_\theta)$ 
21:      $\hat{Y} \leftarrow \hat{Y} \cup y$ 
22:   end while
23: end function

```

node features for enhancing GNNs performance. We begin by describing the experimental setup and then present detailed results. Additionally, we visualize predictions before and after reconstruction to assess the impact of our method on GNN predictions. Finally, we analyze the validity of the neural Lyapunov function through visualizations.

Experimental Setup

Base Model We chose SGC (Wu et al. 2019) as our base model. SGC is a simple graph neural network that reduces the multi-layer convolution operations of GCN (Kipf and Welling 2017) to single matrix multiplication, making it more efficient. Our method requires using an SMT solver to identify states that violate Lyapunov constraints, so we must keep the SMT solving time within an acceptable range. Thus, we select SGC as the base model to accelerate the solving process by reducing the graph neural network's parameters.

Datasets We evaluate our method on five popular graph datasets: Cora, Citeseer, Pubmed (Yang, Cohen, and Salakhutdinov 2016), Amazon Photo, and Amazon Computers (Shchur et al. 2019). These datasets are standard benchmarks for semi-supervised node classification tasks. The statistics of these datasets are summarized in Appendix C. For each dataset, we follow the setup from FRGNN (Ding et al. 2024) and apply the Scalable Biased Sampler (Zhu et al. 2021) to create training, validation, and test sets. This sampling method effectively captures datasets with distri-

Table 1: Results(%) for the semi-supervised node classification task on the four datasets. Training split represents the method for selecting training nodes. ‘Bias’ means that training nodes are selected using the Scalable Biased Sampler (Zhu et al. 2021). Biased training samples simulate the situation with distribution shift. Each result is reported as an average \pm standard deviation across 10 experiments. The footnote of FRGNN indicates the base model of FRGNN. * indicates that the FRGNN only replaces one class of node features. OOM indicates that the method runs out of memory. The best results are highlighted in bold and the second-best results are underlined.

Method(Year)	Training split	Cora	Citeseer	Pubmed	Photo	Computers
SGC(2019)	Bias	64.36 ± 2.90	60.46 ± 2.06	50.68 ± 3.00	83.69 ± 0.37	69.35 ± 0.20
MH-AUG(2021)	Bias	62.98 ± 4.05	61.40 ± 1.08	51.31 ± 4.02	84.44 ± 3.71	69.74 ± 2.56
KDGA(2022)	Bias	66.27 ± 2.82	57.63 ± 3.01	OOD	OOD	OOD
FRGNN [*] _{SGC} (2024)	Bias	64.89 ± 3.08	60.97 ± 1.89	51.27 ± 3.28	84.73 ± 0.27	69.28 ± 0.34
FRGNN [*] _{GCN} (2024)	Bias	65.12 ± 2.89	61.02 ± 2.33	52.37 ± 2.69	84.21 ± 0.35	69.59 ± 0.22
FRGNN [*] _{APPNP} (2024)	Bias	67.06 ± 1.84	62.39 ± 1.72	51.13 ± 3.78	82.32 ± 0.76	70.21 ± 0.21
Ours _{NC}	Bias	67.22 ± 2.27	62.54 ± 1.82	52.90 ± 2.91	84.96 ± 0.29	70.64 ± 0.19

Table 2: Classification accuracy comparison between our neural controller and traditional controller on three datasets. Each result is reported as an average \pm standard deviation across 10 experiments. MFAC indicates that the controller is MFAC and NC indicates that the controller is our neural controller. The best results are highlighted in bold.

Method	Cora	Citeseer	Pubmed
SGC	64.36 ± 2.90	60.46 ± 2.06	50.68 ± 3.00
Ours _{MFAC}	63.13 ± 3.42	56.73 ± 3.80	51.97 ± 2.78
Ours _{NC}	67.22 ± 2.27	62.54 ± 1.82	52.90 ± 2.91

bution shifts, allowing us to demonstrate the ability of our method to address such issues.

Implementation Details Our training process for the neural controller and the neural Lyapunov function heavily relies on generating counterexamples, which necessitates ensuring the speed of the SMT solver. Since the speed of SMT solver is proportional to the number of parameters in each graph neural network layer, we downsample the node features to reduce the parameter count. We apply PCA to reduce the feature dimensions to a fixed 20 dimensions, making it the input size for all experiments. We use SGC as the base model, setting its steps of feature propagation to 3 and its output size to the number of classes. Our neural controller f_θ is a two-layer MLP with a hidden size of 16. Our neural Lyapunov function V_ϕ is also a two-layer MLP with a hidden size of 16 and an output size of 1. We train both f_θ and V_ϕ using the Adam optimizer with a learning rate of 0.001. We conduct all experiments on an RTX 3090 24G GPU. More details are provided in the Appendix B.

Baseline We select MH-AUG (Park et al. 2021), KDGA (Wu et al. 2022), and FRGNN (Ding et al. 2024) as the baselines. More detail about these methods is provided in the Appendix D.

We also compare our neural controller with traditional controllers. PID and LQR are not suitable for this system due to the complex nonlinearity of GNNs. We adopt the MFAC

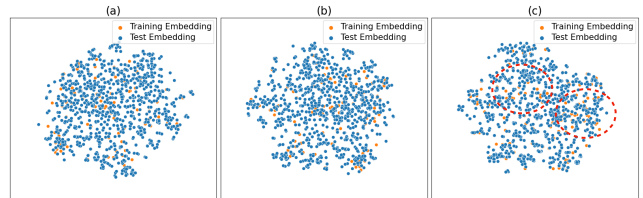


Figure 3: Visualization of the Cora dataset after dimensionality reduction with t-SNE. (a) Node embeddings derived from the original node features; (b) Node embeddings derived from the reconstructed node features by FRGNN; (c) Node embeddings derived from the reconstructed node features by our method. Orange points represent the training node embeddings, while blue points depict the test node embeddings. The red dashed line highlights that our method effectively aligns the embeddings of test nodes more closely with those of the training nodes compared to the original GNN and FRGNN.

as the controller for test-time feature reconstruction.

Results

Performance Comparison We evaluated our method on the Cora, Citeseer, Pubmed, Amazon Photo, and Amazon Computers datasets, with results shown in Table 1. Our approach outperformed SGC across all datasets, demonstrating its effectiveness and robustness across different statistical characteristics.

Unlike MH-AUG and KDGA, which improve robustness by augmenting data during training, our method enhances robustness by reconstructing features during the testing phase. Our approach consistently achieved superior performance on all datasets compared to MH-AUG and KDGA, indicating the benefits of feature reconstruction at test time.

We further compare our method with FRGNN. FRGNN trains an MLP with GNN predictions and node features to generate class representative embeddings. This paradigm makes FRGNN dependent on the Lipschitz condition, which imposes strict requirements on the MLP’s training data. If

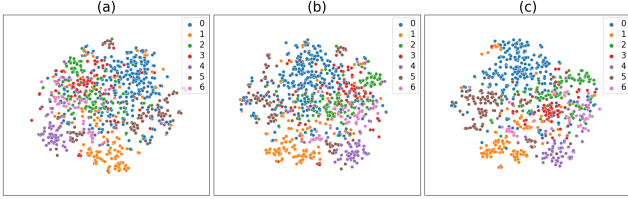


Figure 4: Visualization of the Cora dataset after dimensionality reduction with t-SNE. (a) Node embeddings derived from the original node features; (b) Node embeddings derived from the reconstructed node features by FRGNN; (c) Node embeddings derived from the reconstructed node features by our method. Different colors indicate different categories. Our method shows better clustering of node embeddings for each class than the original GNN and FRGNN.

GNN predictions deviate significantly from the ground truth, it may struggle to find suitable class representative embeddings. Our approach formalizes the graph neural network as a control system and reconstructs node features through a neural controller to ensure the new predictions close to the ground truth. The node features reconstructed by our method can better satisfy the definition of class representative embeddings than FRGNN. Therefore, when replacing the features of a single class of labeled nodes, our method outperforms FRGNN on all datasets.

To further demonstrate the effectiveness of our controller, we compare it with traditional controllers on three datasets, as shown in Table 2. For such a control system with complex nonlinearity and coupling, MFAC fails to find the class representative embeddings, leading to a significant performance drop. Our neural controller outperforms MFAC on all datasets, indicating the superiority of neural controllers in adjusting node features for GNNs.

Visualization To illustrate the performance gains in classification from replacing node features, we conduct a t-SNE visualization of node embeddings on the Cora dataset, as shown in Figure 3. The figure displays the original node embeddings, those reconstructed by FRGNN, and those reconstructed by our method. In this visualization, blue points represent test nodes and orange points represent training nodes. The results in this figure demonstrate that our method effectively aligns the embeddings of test nodes more closely with those of the training nodes compared to the original GNN and FRGNN scenarios. This alignment reduces the distribution shift between training and test nodes, enhancing the ability of the classifier to accurately categorize embeddings. Therefore our method achieves better classification performance on test nodes. We also visualize the embeddings for each node class in Figure 4, where our approach shows better clustering of node embeddings for each class than FRGNN.

To further analyze the Lyapunov function, we visualize its values on the Cora dataset, as shown in Figure 5. We sample vectors near the equilibrium point and calculate their corresponding Lyapunov function values. We reduce these vectors and the equilibrium point to two dimensions for visu-

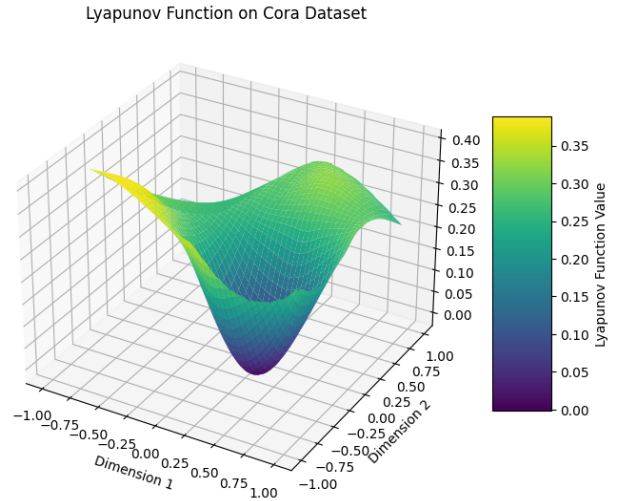


Figure 5: Visualization of Lyapunov function value. Dimension 1 represents dimension 1 of the t-SNE reduced state, Dimension 2 represents dimension 2 of the t-SNE reduced state, and the color represents the value of the Lyapunov function. The Lyapunov function values are zero near the equilibrium point and increase as they move away, indicating that the learned neural Lyapunov function meets the Lyapunov stability criterion.

alization with t-SNE. Dimension 1 and Dimension 2 represent the reduced dimensions and the vertical axis shows the Lyapunov function values. The Lyapunov function values are zero near the equilibrium point and increase as they move away, indicating that our Lyapunov function meets the Lyapunov stability criterion. This phenomenon confirms that our controller can maintain the system output near the equilibrium point (i.e., ground truth).

Conclusion

In this paper, we propose a novel testing-time feature reconstruction method to enhance the robustness of graph neural networks to distribution shifts. We formalize GNNs as a control system, treating node features as controlled variables. By designing a neural controller to reconstruct these node features, we ensure that the predictions gradually stabilize near the ground truth. We introduce a neural Lyapunov function to aid in controller training, ensuring system stability and obtaining class representative embeddings. We evaluate our method across multiple datasets, demonstrating its effectiveness in reconstructing node features and enhancing GNN performance.

Limitation: currently, the solving time of the solver remains a bottleneck for our method. We have to downsample the node features to reduce the number of parameters in the graph neural network, which may affect the model performance. In the future, we will explore more efficient methods to solve the Lyapunov constraints.

References

Ang, K. H.; Chong, G.; and Li, Y. 2005. PID control system analysis, design, and technology. *IEEE Transactions on Control Systems Technology*, 13(4): 559–576.

Buffelli, D.; Liò, P.; and Vandin, F. 2022. Sizeshiftreg: a regularization method for improving size-generalization in graph neural networks. *Advances in Neural Information Processing Systems*, 35: 31871–31885.

Chang, Y.; Roohi, N.; and Gao, S. 2020. Neural Lyapunov Control. *CoRR*, abs/2005.00611.

Dai, H.; Landry, B.; Yang, L.; Pavone, M.; and Tedrake, R. 2021. Lyapunov-stable neural-network control. *CoRR*, abs/2109.14152.

Ding, K.; Xu, Z.; Tong, H.; and Liu, H. 2022. Data augmentation for deep graph learning: A survey. *ACM SIGKDD Explorations Newsletter*, 24(2): 61–77.

Ding, R.; Yang, J.; Feng, J.; Zhong, X.; and Xie, L. 2024. FR-GNN: Mitigating the Impact of Distribution Shift On Graph Neural Networks via Test-Time Feature Reconstruction. *IEEE Internet of Things Journal*, 1–1.

Fan, S.; Wang, X.; Shi, C.; Cui, P.; and Wang, B. 2023. Generalizing graph neural networks on out-of-distribution graphs. *IEEE Transactions on Pattern Analysis and Machine Intelligence*.

Gu, W.; Valavanis, K. P.; Rutherford, M. J.; and Rizzo, A. 2020. UAV model-based flight control with artificial neural networks: A survey. *Journal of Intelligent & Robotic Systems*, 100(3): 1469–1491.

Hou, Z.; and Xiong, S. 2019. On model-free adaptive control and its stability analysis. *IEEE Transactions on Automatic Control*, 64(11): 4555–4569.

Jiang, F.; Pourpanah, F.; and Hao, Q. 2020. Design, Implementation, and Evaluation of a Neural-Network-Based Quadcopter UAV System. *IEEE Transactions on Industrial Electronics*, 67(3): 2076–2085.

Jin, W.; Zhao, T.; Ding, J.; Liu, Y.; Tang, J.; and Shah, N. 2023. Empowering Graph Representation Learning with Test-Time Graph Transformation. *arXiv*:2210.03561.

Kim, B.-S.; and Calise, A. J. 1994. Nonlinear flight control using neural networks. *Journal of Guidance Control and Dynamics*, 20: 26–33.

Kipf, T. N.; and Welling, M. 2017. Semi-Supervised Classification with Graph Convolutional Networks. In *International Conference on Learning Representations (ICLR)*.

Kwakernaak, H.; and Sivan, R. 1972. *Linear Optimal Control Systems*. USA: John Wiley & Sons, Inc. ISBN 0471511102.

Li, H.; Wang, X.; Zhang, Z.; and Zhu, W. 2022. Out-of-distribution generalization on graphs: A survey. *arXiv preprint arXiv:2202.07987*.

Park, H.; Lee, S.; Kim, S.; Park, J.; Jeong, J.; Kim, K.-M.; Ha, J.-W.; and Kim, H. J. 2021. Metropolis-Hastings Data Augmentation for Graph Neural Networks. In *Advances in Neural Inf. Proc. Syst.*, 19010–19020.

Qin, Y.; Wang, X.; Zhang, Z.; Xie, P.; and Zhu, W. 2022. Graph neural architecture search under distribution shifts. In *International Conference on Machine Learning*, 18083–18095. PMLR.

Shchur, O.; Mumme, M.; Bojchevski, A.; and Günnemann, S. 2019. Pitfalls of Graph Neural Network Evaluation. *arXiv*:1811.05868.

Sui, Y.; Wu, Q.; Wu, J.; Cui, Q.; Li, L.; Zhou, J.; Wang, X.; and He, X. 2024. Unleashing the power of graph data augmentation on covariate distribution shift. *Advances in Neural Information Processing Systems*, 36.

Wu, F.; Souza, A.; Zhang, T.; Fifty, C.; Yu, T.; and Weinberger, K. 2019. Simplifying Graph Convolutional Networks. In *Proceedings of the 36th International Conference on Machine Learning*, 6861–6871. PMLR.

Wu, L.; Lin, H.; Huang, Y.; and Li, S. Z. 2022. Knowledge Distillation Improves Graph Structure Augmentation for Graph Neural Networks. In *Advances in Neural Inf. Proc. Syst.*, 11815–11827.

Wu, Z.; Pan, S.; Chen, F.; Long, G.; Zhang, C.; and Philip, S. Y. 2020. A comprehensive survey on graph neural networks. *IEEE transactions on neural networks and learning systems*, 32(1): 4–24.

Yang, Z.; Cohen, W. W.; and Salakhutdinov, R. 2016. Revisiting semi-supervised learning with graph embeddings. In *Proceedings of the 33rd International Conference on International Conference on Machine Learning - Volume 48*, ICML'16, 40–48. JMLR.org.

Yuan, H.; Yu, H.; Gui, S.; and Ji, S. 2022. Explainability in graph neural networks: A taxonomic survey. *IEEE transactions on pattern analysis and machine intelligence*, 45(5): 5782–5799.

Zhou, R.; Quartz, T.; Sterck, H. D.; and Liu, J. 2022. Neural Lyapunov Control of Unknown Nonlinear Systems with Stability Guarantees. In Oh, A. H.; Agarwal, A.; Belgrave, D.; and Cho, K., eds., *Advances in Neural Information Processing Systems*.

Zhu, Q.; Ponomareva, N.; Han, J.; and Perozzi, B. 2021. Shift-robust gnns: Overcoming the limitations of localized graph training data. *Advances in Neural Information Processing Systems*, 34.